Materials Science in Semiconductor Processing 186 (2025) 109039

Contents lists available at ScienceDirect

Materials Science in Semiconductor Processing

journal homepage: www.elsevier.com/locate/mssp

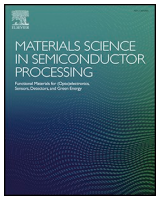

Correlation of reverse dark current-voltage characteristics and gamma detection properties of a p-CdTe/n-CdTe/n^+-Si vertical diode-type radiation detector

M. Niraula *, I. Torimoto, R. Okumura

Nagoya Institute of Technology, Graduate School of Engineering, Gokiso, Showa, Nagoya, 466-8555, Japan

ARTICLE INFO

Keywords:
Gamma ray detectors
CdTe epitaxial layer
Single crystal
Diode-type detector
Dark current
Dislocation density

ABSTRACT

The reverse dark current mechanism of a p-CdTe/n-CdTe/n^+-Si vertical diode-type gamma ray detector, fabricated by growing epitaxial CdTe on Si substrates was studied and corelated with the detector's gamma detection properties. The detector dark current deviated from the Shockley-Reed-Hall (SRH) generation mechanism but showed tunneling was the dominant process. The dark current was strongly controlled by the dislocation densities and their distribution in the CdTe epilayer. Detectors that exhibited poor gamma detection properties had high dislocation densities and had large and nearly temperature independent dark currents. Good working detectors, on the other hand, showed small dark currents with a clear temperature dependence. These working detectors, fabricated with optimized crystal growth techniques, had a dislocation density nearly an order of magnitude lower than those of non-working or poorly working detectors.

1. Introduction

The epitaxial growth of thick CdTe single crystals on Si substrates is a promising method, as it provides large, uniform crystals ideal for X-ray or infrared imaging sensors applications. Additionally, this technique opens the possibility of monolithic integration of such devices on a Si-based platform [1–3]. However, material dissimilarities between CdTe and Si, such as large lattice and thermal expansion mismatch, and polarity differences, lead to high density of defects, such as threading dislocations and twinning [4–6]. These defects significantly degrade the device performance rendering them unsuitable for their intended applications. By carefully controlling the substrate preparation and by applying very stringent growth conditions, we successfully achieved twin-free single crystals of CdTe on the Si substrates using metalorganic vapor phase epitaxy (MOVPE) growth [2,7]. We further utilized these single crystals to fabricate energy resolving X-ray detectors in a p-CdTe/n-CdTe/n^+-Si heterojunction diode structure by successively growing an iodine-doped n-CdTe, and then an undoped p-like CdTe on a (211)-oriented n^+-Si substrate [2,8,9]. This is a vertical-type device which operates in a reverse bias mode, where photo-generated charge carriers travel across the junction and collected the respective electrodes. Although most of the detectors fabricated demonstrated their energy discriminating capabilities by detecting and resolving energy peaks from a gamma source, other detectors failed to resolve any energy peaks. Nonetheless, energy resolving properties of the detectors were still inferior compared to the standard melt-grown bulk CdTe planar or Schottky type detectors [8–10]. It was found that our detectors had large reverse biased dark (leakage) currents, presumably due to high dislocation densities, that degraded the detectors performances [8,9]. Dislocations are generated during the crystal growth due to the large lattice constant mismatch and thermal expansion coefficient mismatch between the Si substrate and the CdTe epilayer. Furthermore, the device dark currents did not follow the simple Shockley-Reed-Hall (SRH) generation-recombination(G-R) mechanism. The dark current values and their dependences with the applied reverse biases were different in the working and the non-working or the poorly working one. Hence, understanding the mechanism of dark current flow in our detectors and suppressing their values were needed to obtain good working detector for practical applications.

In the present study, we have investigated dark current flow mechanism in our detectors fabricated using different growth processes and correlated with the detector's gamma detection properties. It was suggested that electrically active defects, mainly threading dislocations in the epilayer and their energy level and spatial distribution were the

* Corresponding author.
E-mail address: m.niraula@nitech.ac.jp (M. Niraula).

https://doi.org/10.1016/j.mssp.2024.109039
Received 10 September 2024; Received in revised form 8 October 2024; Accepted 21 October 2024
Available online 29 October 2024

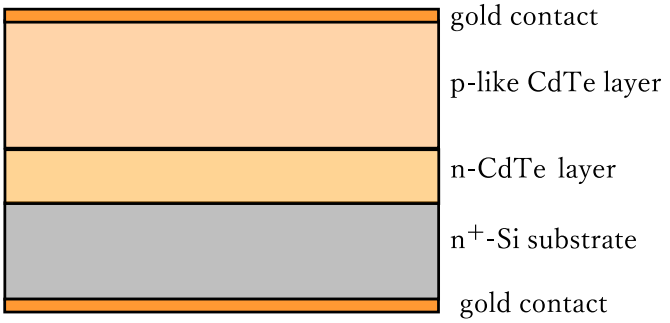

Fig. 1. Schematic cross-sectional drawing of the detector studied. Depending on the n-CdTe and the p-CdTe growth techniques, the detectors were named D1, D2 and D3 as detailed in Table 1.

Table 1
Fabrication details for D1 to D3 detectors.

Detector ID	n-CdTe growth details	p-CdTe growth details	**Total CdTe thickness (μm)**
D1	3h growth, anneal, 2h growth	4h continuous	45 ± 2
D2	5h continuous growth	(1h x 4) growth interruption	45 ± 2
D3	3h growth, anneal, 2h growth	(1h x 4) growth interruption anneal at each stage	45 ± 2

main cause of observed dark current variations, thereby deteriorating the detector's properties. Reducing the dislocation density in the CdTe epilayers by optimizing the crystal growth technique, detectors with good gamma detection properties could be obtained.

2. Experimental details

Thick single crystal CdTe epilayers were grown directly on (211) n^+-Si substrates using a metalorganic vapor phase epitaxy (MOVPE) growth technique. The growth details are already reported [7–9]. A specialized Si substrate pretreatment was developed that allowed us to achieve a direct growth of CdTe on the Si substrates without introduction of the intermediate buffer layers such as ZnTe or Ge [7–9]. Detectors were fabricated in a p-CdTe/n-CdTe/n^+-Si heterojunction diode structure by growing an iodine-doped n-CdTe and then undoped p-CdTe successively on the n^+-Si substrates. Planar type gold contacts were evaporated on the top p-CdTe side and on the backside of the n^+-Si substrates. The p-CdTe was slightly etched in a bromine-methanol solution, whereas the back side of the Si substrates were subjected to a mechanical polishing and etching prior to the gold contact deposition to make the Ohmic contact. Fig. 1 shows a schematic cross-sectional diagram of the detector studied. The n-CdTe was grown at 325 °C, with the total thickness of 5 μm and the electron concentration of $5x10^{17}$ cm^{-3}. The total thickness of p-CdTe layer was typically 40 μm thick, grown at 450 °C without intentional doping, however, exhibits a p-type conductivity [11]. Three types of detectors - named D1, D2 and D3 were investigated. In these detectors the crystal growth temperature, doping conditions, thicknesses of the n-CdTe and the p-CdTe, and detector fabrication techniques were kept similar. However, introduction of the growth interruptions during the crystal growth and the annealing of the crystals during growths were varied as detailed in Table 1. In the growth interruption technique, after growing CdTe crystal for some fixed time the growth is stopped, and the substrate temperature is decreased to 100 °C, before restarting the growth and the process is repeated till the final thickness is reached. In case of annealing, after interrupting the growth the substrate temperature is raised to 550 °C for 5 min before setting the substrate

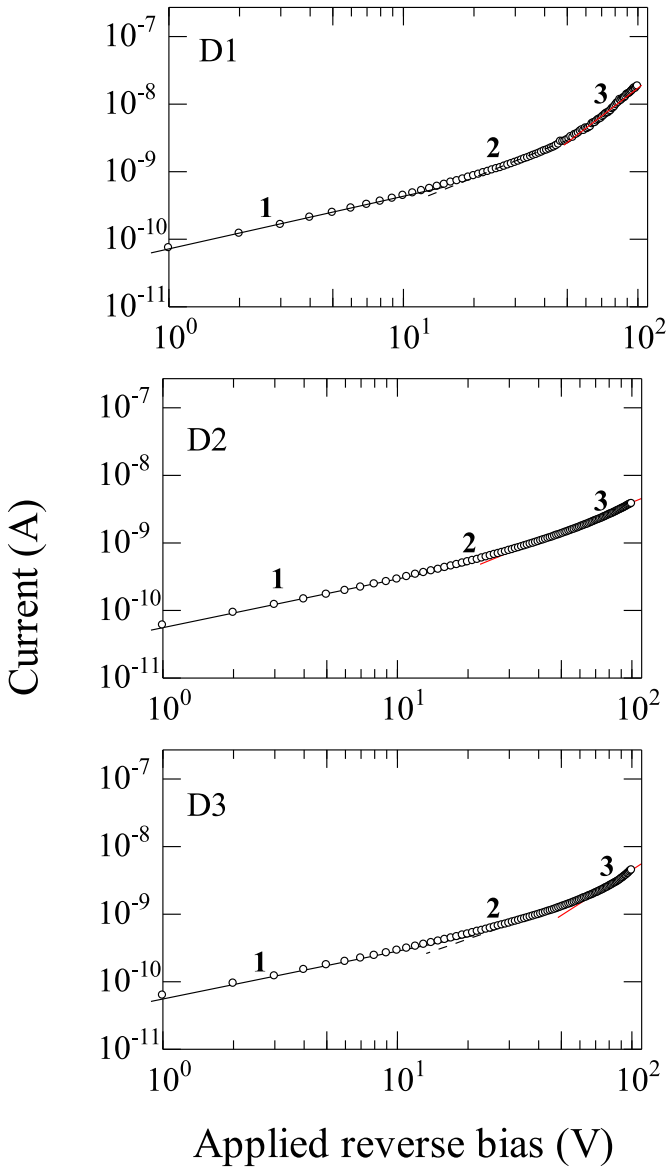

Fig. 2. Reverse biased *I-V* characteristics of detectors (D1-D3) measured in dark at room-temperature. The numbers in the figure indicated the region where the slopes of the curve changes.

temperature to the growth temperature for subsequent growths. These techniques were previously studied which help to reduce dislocation densities and yields epilayers with improved crystallinity and uniformity [12].

Crystallinity of these samples were also evaluated using double crystal X-ray rocking curve (DCRC) using a Rigaku SmartLab diffractometer. Dislocations decorative etch pit technique using an Everson solution with a volumetric ratio of lactic acid/nitric acid/hydrofluoric acid of 25:4:1 was employed to estimate the dislocation density [13]. The samples were etched for a fixed etching time of 2 min, and the triangular pits formed on the CdTe surfaces were counted using an optical microscope.

All detectors were further diced into 2 mm square chip for electrical characterization. The current-voltage (*I-V*) measurement was performed in a dark condition at room temperature and also by varying the temperature from −30 °C to 20 °C on a probe-test station integrated with an Agilent power device analyzer and a thermal control system. For the radiation measurements, the detectors were mounted on a metal-can package and wire bonded. This assembly was then plugged into the

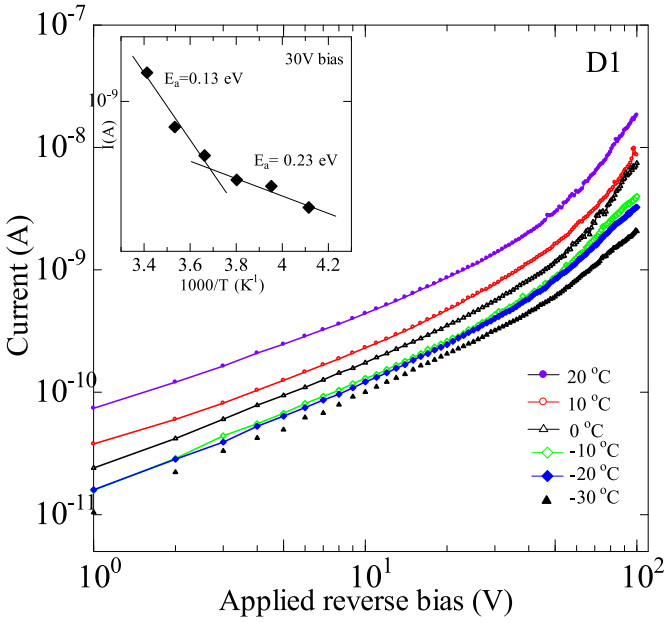

Fig. 3. Reverse dark currents of detector D1 measured at different temperatures. The inset in the figure is the Arrhenius plot of dark currents at 30 V reverse bias.

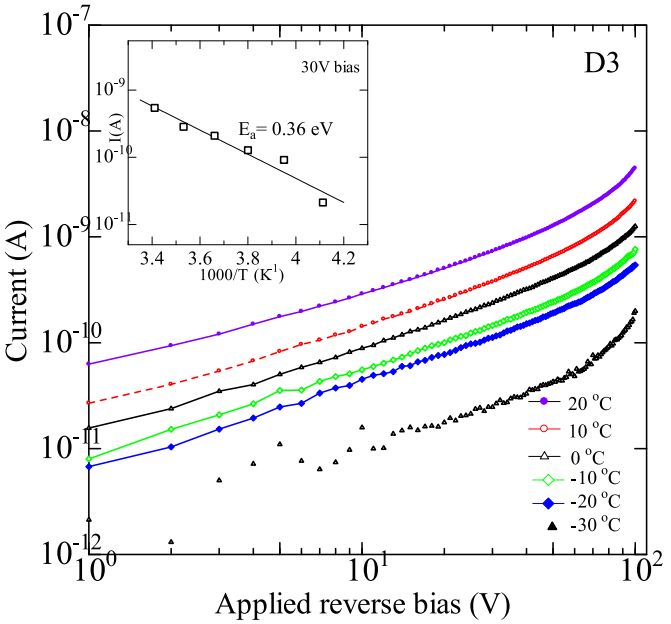

Fig. 5. Reverse dark currents of D3 detector measured at different temperatures. The inset in the figure is the Arrhenius plot of dark currents at 30 V reverse bias.

dedicated radiation measurement system consisting of a pre-amp, shaping amp and multichannel analyzer. Radiation measurement was performed at room temperature using a ^{241}Am gamma source, under identical conditions for all detectors.

3. Results and discussion

Fig. 2 shows the reverse biased *I-V* characteristics of detectors measured in dark at room-temperature, by applying a positive bias on the backside electrode on the n^+-Si substrate. The value of dark current is high in D1 detectors when compared to the D2 and the D3 detectors. The later detectors, on the other hand, showed almost similar values of dark currents at all biases investigated. To analyze the dependence of dark current on the applied bias, linear regions in the data in Fig. 2 were fitted with straight lines to determine the slopes. The results show the dark current in all detectors does not follow the square-root dependence with the applied voltage as expected in a p-n junction diode. Three different regions in the figure were designated as 1 through 3 according to their slopes. The slopes were found to be 0.85 in D1, and 0.75 in D2 and D3 detectors in low voltage region. This changes to 1.0 in D1 and D2, while 1.36 in D3 in the mid voltage range and then 1.96 in D1 and 1.6 in D2 and D3 detectors in high voltage range.

To analyze the dark current mechanism, temperature dependence of the dark current was studied. The reverse dark currents of all three

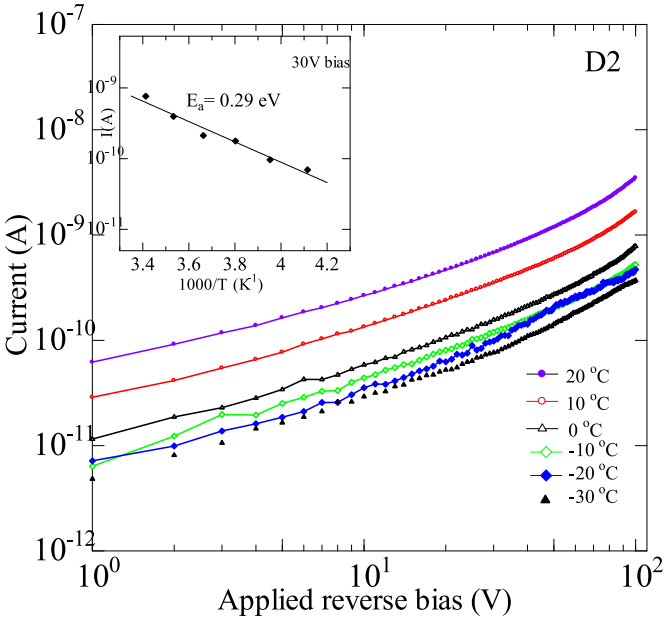

Fig. 4. Reverse dark currents of D2 detector measured at different temperatures. The inset in the figure is the Arrhenius plot of dark currents at 30 V reverse bias.

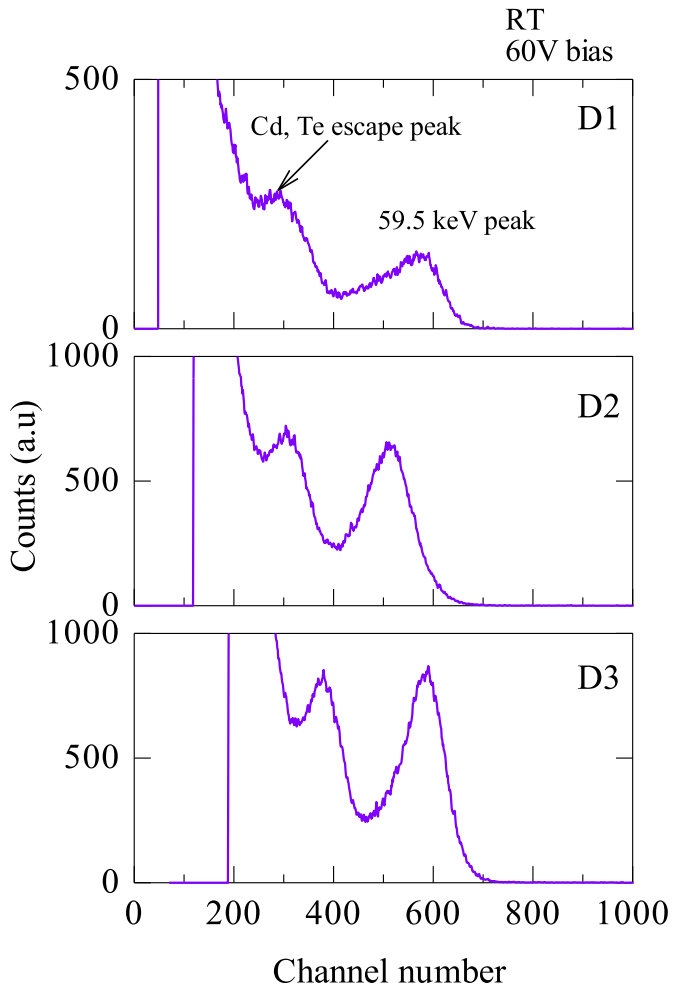

Fig. 6. Comparison of the pulse height spectrum of the ^{241}Am gamma source obtained from detectors D1-D3. All detectors were biased at 60V and operated at room temperature. All other measurement conditions were also kept similar during the measurement.

detectors were evaluated by varying the temperature from 20 °C to −30 °C, and the results are plotted in Figs. 3–5. Compared to other detectors, the D1 detector exhibited different characteristics as in Fig. 3. The dark current increase gradually with applied bias. For a given applied bias, the dark current increases as the temperature increases, however, the increment is moderate. An Arrhenius plot of the dark current at 30V as a function of temperature is also shown in Fig. 3(inset). However, the data could not be fitted with a single activation energy. The activation energy was 0.23 eV below 0 °C range, which decreases to 0.13 eV in the temperature range above 0 °C. Moreover, the activation energy varied with the applied bias. The D2 detector as in Fig. 4 showed both the voltage and the temperature dependences of dark current. However, the temperature dependence of the dark current was less prominent in the temperature range from −10 °C to −30 °C. Shown in the inset of Fig. 4 is the Arrhenius plot of the dark current at an applied bias of 30V, which gives an activation energy of 0.29 eV. The value of the activation energy was almost similar for other applied biases. Likewise, the D3 detector as in Fig. 5 exhibited both the voltage and temperature dependences of dark currents. The temperature dependence of dark current in this detector was strong compared to the other two detectors (D1 and D2). The activation energy of the dark current calculated at an applied bias of 30V (Fig. 5, inset) was 0.36 eV and like in D2 detector, variation of activation energies with applied bias was small. The observed results of the temperature and the field dependence (current not varying with square-root of applied voltage) of these detectors (D1-D3) suggest the dark current is not due to the Shockley-Reed-Hall (SRH) generation mechanism, but other processes such as band-to-band tunneling and trap-assisted tunneling (TAT) could be the dominant mechanisms for the current flow [14–17]. In band to band tunneling, an electron tunnels from the valence band into the trap and then tunnels from the trap to the conduction band. In TAT, it could be tunneling from the valence band to the trap and thermal excitation from the trap into the conduction band, or thermal excitation from the valence band to the trap and then tunneling or thermal excitation from the trap to the conduction band. The small temperature dependence, particularly at low-temperature region, coupled with activation energies smaller than the half of the band-gap energy of CdTe ($E_a < E_g/2$) suggest band-to-band tunneling, followed by the TAT could be the possible mechanisms in D1 and D2 detectors [14–17]. On the other hand, the strong temperature dependence in D3 detector suggests the TAT could be the main case [14–17].

Fig. 6 shows the gamma detection properties of the detectors. The measurement was performed at room-temperature by applying a positive bias of 60V on the back side of the n^+-Si substrate (reverse bias). Gamma rays from an ^{241}Am radioisotope were irradiated from the p-CdTe side, and signal generated was collected through the n^+-Si side. All measurement conditions were kept unchanged during D1 through D3 detector evaluation. The result shows all detectors can detect the 59.5 keV main gamma peak from the ^{241}Am source, and the Cd and the Te escape peaks which are merged into a single peak. However, the gamma

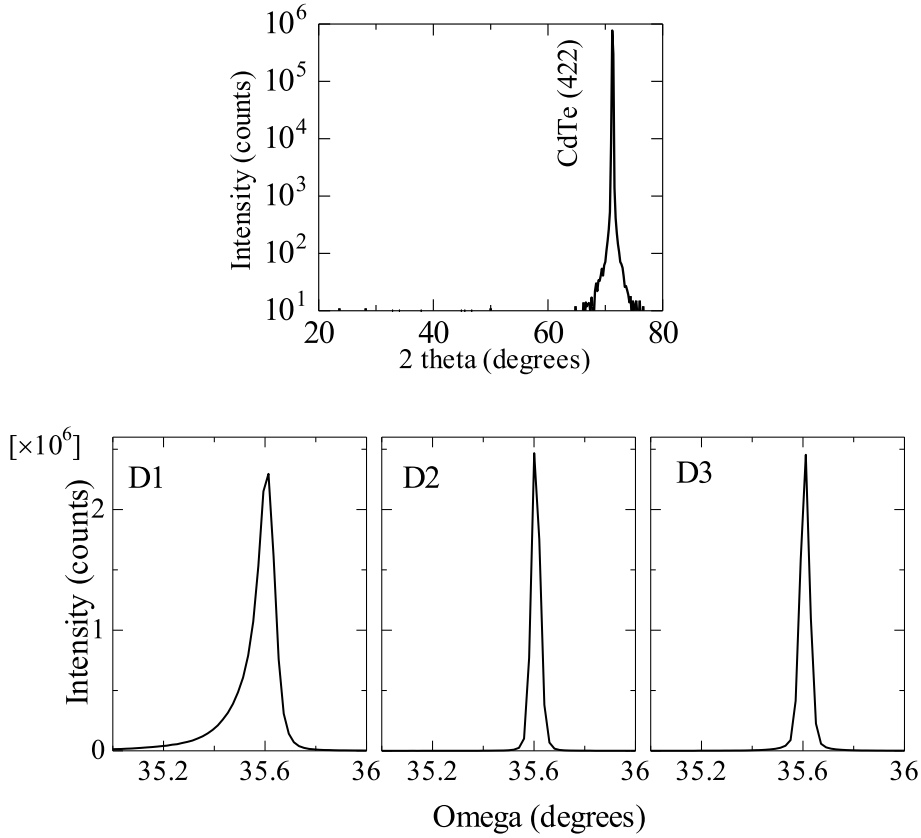

Fig. 7. Typical XRD pattern of CdTe epitaxial layer on (211) Si substrate (top), and XRD (422) rocking curve of D1 to D3 samples (bottom).

detection property of the D1 detector is inferior. The main peak detected is broad and less pronounced with a long lower energy tail. On the other hand, the detection property improves significantly in D2 and D3 detectors, where the peak shape gets narrower and distinct, and the lower energy tailing is reduced. Despite improved peak shape with less tailing, the peak position of D2 detector is at lower channel than the other two detectors indicating incomplete charge collection. It could be due to the statistical variation or due to incomplete depletion of the detector, which needed further verification.

The best response was obtained in the D3 detector, where the shape of the main peak gets very distinct and nearly symmetrical. This indicates the improved charge transport properties of the D2 and D3 detectors. This could be related the lesser densities of trapping centers in these detectors resulted due to the decrease of the threading dislocation densities compared to the D1 detector. Furthermore, the lower dark current suppresses the electronic noise of the measurement system, resulting the improved performance.

To verify this, we examined crystallinity of these detectors using X-ray diffraction (XRD) and further estimated the dislocation density by etch pit analysis technique. The results are shown in Figs. 7 and 8, respectively. The typical XRD pattern of our CdTe layers shown in Fig. 7 exhibits single diffraction peak corresponding to CdTe (422) reflection, indicating the crystal is monocrystalline with grown orientation parallel to the (211)Si substrate. The X-ray rocking curve analysis revealed that the full width of half-maximum (FWHM) value was 320, 200 and 155 arcsec for the D1, D2 and D3 samples respectively, suggesting the crystallinity of D2 and D3 detectors are better compared to the D1 detector. Shown in Fig. 8 is the surface morphology of Everson etched samples. The etch pit density counted from these sample surfaces was $2x10^6$, $4x10^5$, and $1x10^5$ cm^{-2} for D1, D2 and the D3 detectors, respectively, which corelate well with the observed DCRC values, suggesting improvement in crystallinity. Introduction of growth interruption and annealing during crystal growth in D2 and D3 detectors promote the dislocation movement due to the imposed thermal stress, assisting coalescence or annihilation of the dislocations and hence reduce their density [5,18]. This results in improved crystallinity of D2 and D3 compared to the D1, which was not subjected to these techniques during growth. Furthermore, the best crystallinity in D3 indicates that annealing subjected at the early stage of growth, followed by growth interruption and annealing (see Table 1) is more effective in dislocation reduction than the growth interruption alone. The smaller dark currents in the D2 and D3 detectors compared to that of the D1 detector could be related to lesser dislocation densities in these detectors. The variation of current transport mechanism could be due to the non-uniform distribution of dislocations, where regions with higher dislocation density contains high concentration of trapping centers. Also, the possibility of dislocations threading the p-n junction which act as shunt leakage path could be the case in D1 detector that exhibit maximum and nearly temperature independent dark current among the detectors studied.

4. Conclusion

Detailed analysis of reverse dark currents of p-CdTe/n-CdTe/n^+-Si vertical diode-type gamma radiation detectors were made and corelated them with the detector's gamma detection properties. The dark current-voltage characteristics revealed the dark current deviated from the simple SRH generation mechanism. Detectors with large dark currents that exhibit only field dependence, but little temperature dependence exhibited poor gamma detection property. On the other hand, gamma detection performance markedly improved in detectors that exhibit both field dependence and good temperature dependence of dark currents. The dislocation density in the epilayer could be well corelated with the observed detector dark currents. However, these dislocations do not form a single midgap trap, but form traps distributed non-uniformly in the energy gap. This affects the carrier transport properties, and hence the gamma detection performance.

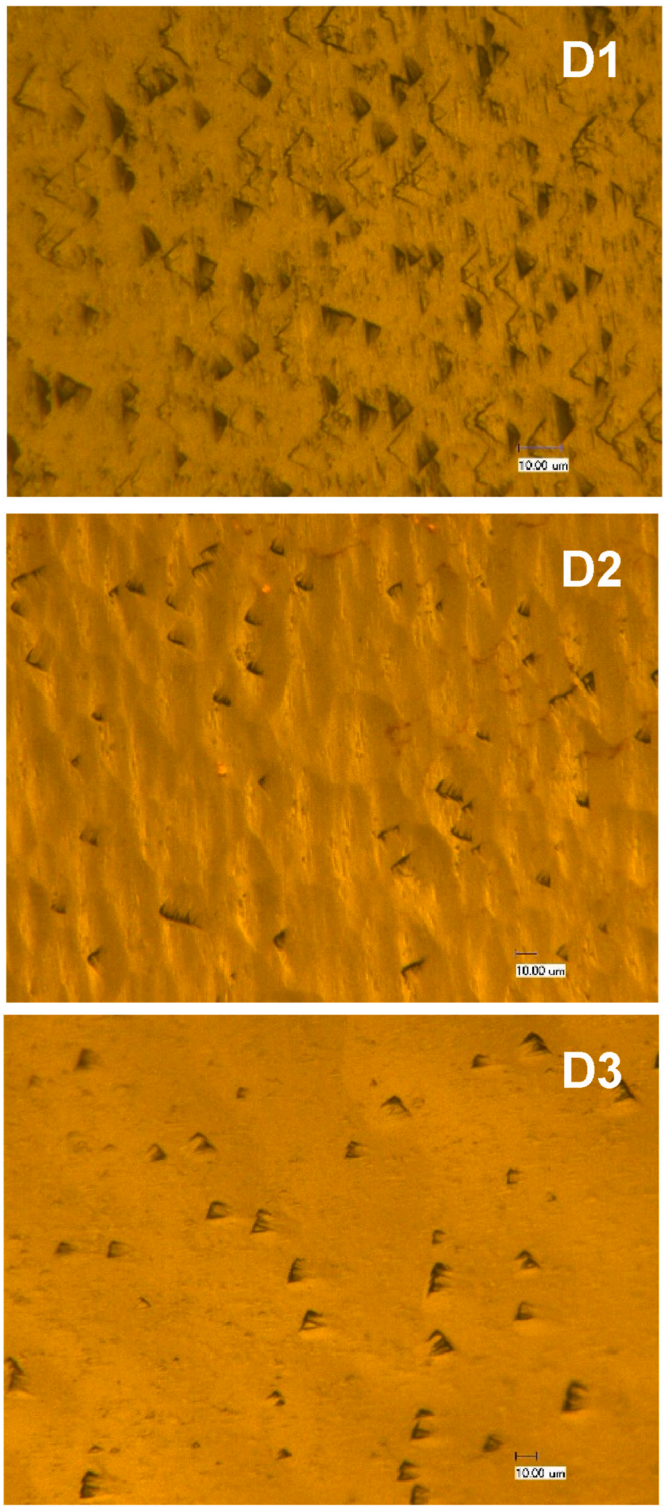

Fig. 8. Surface morphology of D1-D3 samples after Everson etching. The scale bar measures 10 μm in all figures.

Data availability

The data that support the findings of this study are included within the article.

CRediT authorship contribution statement

M. Niraula: Writing – review & editing, Writing – original draft, Methodology, Investigation, Formal analysis, Conceptualization. **I. Torimoto:** Writing – review & editing, Investigation, Data curation. **R. Okumura:** Writing – review & editing, Investigation, Data curation.

Funding source

This research did not receive any specific grant from funding agencies in the public, commercial, or not-for-profit sectors.

Declaration of competing interest

The authors declare that they have no known competing financial interests or personal relationships that could have appeared to influence the work reported in this paper.

References

[1] M. Reddy, X. Jin, D.D. Lofgreen, J.A. Franklin, J.M. Peterson, T. Vang, N. Juanko, F. Torres, K. Doyle, A. Hampp, S.M. Johnson, J.W. Bangs, Demonstration of high-quality MBE HgCdTe on 8-inch wafers, J. Electron. Mater. 48 (2019) 6040–6044.
[2] M. Niraula, K. Yasuda, S. Tsubota, T. Yamaguchi, J. Ozawa, T. Mori, Y. Agata, Characterization of fine-pixel X-ray imaging detector array fabricated by using thick single-crystal CdTe layers on Si substrates grown by MOVPE, IEEE Trans. Electron. Dev. 66 (2019) 518–523.
[3] S. Lee, J.S. Kim, K.R. Ko, G.H. Lee, D.J. Lee, D. Kim, J.E. Kim, H.K. Kim, D.W. Kim, S. Im, Direct thermal growth of large scale Cl-doped CdTe film for low voltage high resolution X-ray image sensor, Sci. Rep. 8 (2018) 14810.
[4] A.J. Stoltz, J.D. Benson, R. Jacobs, P. Smith, A. Almeida, M. Carmody, S. Farrell, P. S. Wijewarnasuriya, G. Brill, Reduction of dislocation density by producing novel structures, J. Electron. Mater. 41 (2012) 2949–2956.
[5] Y. Chen, S. Farrell, G. Brill, P. Wijewarnasuriya, N. Dhar, Dislocation reduction in CdTe/Si ny molecular beam epitaxy through in-situ annealing, J. Cryst. Growth 310 (2008) 5303–5307.
[6] D.J. Smith, S.-C. Tsen, D. Chandrasekhar, P. Crozier, Saroj Rujirawat, G. Brill, Y. Chen, R.t. Sporken, S. Sivananthan, Growth and characterization of CdTe/Si heterostructures: effect of substrate orientation, Mater. Sci. Eng., B 77 (2000) 93–100.
[7] M. Niraula, K. Yasuda, H. Ohnishi, K. Eguchi, H. Takahashi, K. Noda, Y. Agata, J. Cryst. Growth 284 (2005) 15–19.
[8] M. Niraula, K. Yasuda, A. Watanabe, Y. Kai, H. Ichihashi, W. Yamada, H. Oka, T. Yoneyama, H. Nakashima, T. Nakanishi, K. Matsumoto, D. Katoh, Y. Agata, MOVPE growth of CdTe on Si substrates for gamma ray detector fabrication, IEEE Trans. Nucl. Sci. 56 (2009) 836–840.
[9] M. Niraula, K. Yasuda, M. Kojima, S. Kitagawa, S. Tsubota, T. Yamaguchi, J. Ozawa, Y. Agata, Development of large-area CdTe/n+-Si epitaxial layer-based heterojunction diode-type gamma ray detector arrays, EEE Trans. Nucl. Sci. 65 (2018) 1066–1069.
[10] T. Takahashi, T. Mitani, Y. Kobayashi, M. Kouda, G. Sato, S. Watanabe, K. Nakazawa, Y. Okada, M. Funaki, R. Ohno, K. Mori, High-resolution Schottky CdTe diode detector, IEEE Trans. Nucl. Sci. 49 (2002) 1297–1303.
[11] K. Yasuda, M. Niraula, K. Noda, M. Yokota, H. Ohashi, K. Nakamura, M. Omura, I. Shingu, S. Minoura, R. Tanaka, Y. Agata, Development of heterojunction diode-type gamma ray detectors based on epitaxially grown thick CdTe on n+-Si substrates, IEEE Electron. Device Lett. 27 (2006) 890–892.
[12] M. Niraula, K. Yasuda, R. Torii, R. Tamura, Y. Higashira, Y. Agata, Metalorganic vapor phase epitaxy of thick and uniform single crystal CdTe epitaxial layers on (211)Si substrates for X-ray imaging detector development, J. Electron. Mater. 48 (2019) 7680–7685.
[13] J.M. Arias, M. Zandian, S.H. Shin, W.V. McLevige, J.G. Pasko, R.E. DeWames, Dislocation density reduction by annealing of HgCdTe epilayers grown by molecular beam epitaxy on GaAs substrates, J. Vac. Sci. Technol. B 9 (1991) 1646–1650.
[14] A.S. Gilmore, J. Bangs, A. Gerrish, Current voltage modeling of current limiting mechanisms in HgCdTe focal plane array photodetectors, J. Electron. Mater. 34 (2005) 913–921.
[15] L.F. Marsal, J. Pallares, X. Correig, A. Orpella, D. Bardes, R. Alcubilla, Current transport mechanism in n-type amorphous silicon-carbon on p-type crystalline silicon (a-Si0.8C0.2:H/c-Si) heterojunction diodes, Semicond. Sci. Technol. 13 (1998) 1148–1153.
[16] B. Son, Y. Lin, K.H. Lee, Q. Chen, C.S. Tan, Dark current analysis of germanium-on-insulator vertical p-i-n photodetectors with varying threading dislocation density, J. Appl. Phys. 127 (2020) 203105.
[17] S. Krishnamurthy, M.A. Berding, H. Robinson, A. Sher, Tunneling in long-wavelength infrared HgCdTe photodiodes, J. Electron. Mater. 35 (2006) 1399–1402.
[18] W.J. Everson, C.K. Ard, J.L. Sepich, B.E. Dean, G.T. Neugebauer, H.F. Schaake, Etch pit characterization of CdTe and CdZnTe substrates for use in mercury cadmium telluride epitaxy, J. Electron. Mater. 24 (1995) 505–510.